Werry EL, King VA, Barron ML, Banister SD, Sokias R, Kassiou M. Derivatives of the pyrazolo[1,5-a]pyrimidine acetamide DPA-713 as translocator protein (TSPO) ligands and pro-apoptotic agents in human glioblastoma. Eur J Pharm Sci. 2016 Sep 19;96:186-192.

doi: 10.1016/j.ejps.2016.09.026. Epub 2016 Sep 19.

Derivatives of the pyrazolo[1,5-*a*]pyrimidine acetamide DPA-713 as translocator protein (TSPO) ligands and pro-apoptotic agents in human glioblastoma

Eryn L Werry[1], Victoria A. King[2], Melissa L Barron[1], Samuel D. Banister[3], Renee Sokias[3], Michael Kassiou[2,3*]

Faculty of Health Sciences[1], Discipline of Pharmacology[2], School of Chemistry[3], The University of Sydney, Sydney, NSW, Australia

* Corresponding author

E-mail: michael.kassiou@sydney.edu.au; Phone: +612 9351 2745

ABSTRACT

The 18kDa translocator protein (TSPO) is a target for novel glioblastoma therapies due to its upregulation in this cancer and relatively low levels of expression in the healthy cortex. The pyrazolo[1,5-*a*] pyrimidine acetamides, exemplified by DPA-713 and DPA-714, are a class of high affinity TSPO ligands with selectivity over the central benzodiazepine receptor. In this study we have explored the potential anti-glioblastoma activity of a library of DPA-713 and DPA-714 analogues, and investigated the effect of amending the alkyl ether chain on TSPO affinity and functional potential. All ligands demonstrated nanomolar affinity for TSPO, but showed diverse functional activity, for example DPA-713 and DPA-714 did not affect the proliferation or viability of human T98G glioblstoma cells, while the hexyl ether and benzyl ether derivatives decreased proliferation of T98G cells without affecting proliferation in human foetal glial SVGp12 cells. These ligands also induced apoptosis and dissipated T98G mitochondrial membrane potential. This suggests that the nature of the alkyl ether chain of pyrazolo[1,5-*a*] pyrimidine acetamides has little influence on TSPO affinity but is important for functional activity of this class of TSPO ligands.

KEYWORDS: translocator protein, DPA-713, glioblastoma, apoptosis, proliferation

ABBREVIATIONS: BrdU, 5-bromo-2'-deoxyuridine; DMEM/F12, Dulbecco's modified Eagle's medium: Ham's Nutrient Mixture F-12; DMSO, dimethyl sulfoxide; EDTA, ethylenediaminetetraacetic acid; LLE, lipophilic ligand efficiency; MEM, minimum essential medium; PET, positron emission tomography; SPECT, single-photon emission computed tomography; TSPO, translocator protein.

1. INTRODUCTION

Glioblastoma is the most aggressive type of glioma. The current standard of care for glioblastoma involves a combination of aggressive tumor resectioning, radiotherapy and chemotherapy, and produces a median survival rate of 14.2 months (Johnson *et al.*, 2012). Despite the exploration of experimental glioblastoma treatments over the past three decades, the median survival rate has changed only modestly (Omay *et al.*, 2009; Johnson *et al.*, 2012), and identification of early diagnostic methods and improved treatments remains a critical unmet clinical need.

The translocator protein (TSPO), previously named the peripheral benzodiazepine receptor, is an 18 kDa outer mitochondrial membrane protein which is involved in the transport of cholesterol into the mitochondria (Papadopoulos *et al.*, 2006). A range of in vitro and in vivo data implicates TSPO in glioblastoma (Austin *et al.*, 2013; Werry *et al.*, 2015). TSPO expression is positively correlated with in vivo grade and in vitro tumorigenicity in several glioblastoma cell lines, and negatively correlated with glioblastoma survival rate (Miettinen *et al.*, 1995; Veenman *et al.*, 2004; Vlodavsky *et al.*, 2007; Su *et al.*, 2013). Upregulation of TSPO improves the motility and transmigratory capacity of C6 rat glioma cells (Rechichi *et al.*, 2008), and TSPO knockdown decreases the basal proliferative ability of astrocytomas (Chelli *et al.*, 2008). Furthermore, the selective, high affinity TSPO ligand PK 11195 shows cytostatic effects on a range of glioblastoma cell lines (Ikezaki *et al.*, 1990; Zisterer *et al.*, 1998; Chelli *et al.*, 2008; Kugler *et al.*, 2008). The aforementioned studies and the relatively low expression of TSPO in normal cortex (Miyazawa *et al.*, 1998) indicate that TSPO could be a new avenue for molecular imaging and treatment of glioblastoma.

Whilst the isoquinoline carboxamide PK 11195 has been used extensively to study anti-proliferative effects on in vitro glioblastoma, this ligand displays highly variable kinetic behaviour, substantial non-specific binding, and poor bioavailability (Chauveau *et al.*, 2008; Endres *et al.*, 2009), precluding its use as a TSPO-directed glioblastoma therapy or diagnostic agent. Pyrazolo[1,5-*a*] pyrimidine acetamides are a newer chemotype, and although they show reduced affinity to the common TSPO polymorphism rs6971 (Owen *et al.*, 2011), they demonstrate high-affinity for the wild type TSPO and superior selectivity over the central benzodiazepine receptor (Selleri *et al.*, 2001). Two second generation ligands from this class, DPA-713 and DPA-714 (Table 1), show good bioavailability, brain penetrability and stability in humans (Endres *et al.*, 2009; Arlicot *et al.*, 2012; Corcia *et al.*, 2012; Endres *et al.*, 2012; Coughlin *et al.*, 2014). ^{18}(F)-DPA-714 preferentially accumulates in tumours of glioma-bearing rats, and levels correlate with ex vivo assays of TSPO levels in these gliomas, suggesting DPA-714 could be a promising glioblastoma imaging agent (Tang *et al.*, 2012; Winkeler *et al.*, 2012; Awde *et al.*, 2013). DPA-714, but not DPA-713, stimulated pregnenolone release from rat C6

glioma cells (James *et al.*, 2008; Reynolds *et al.*, 2010). Although the role of TSPO in pregnenolone stimulation in vivo has recently been questioned (Banati *et al.*, 2014), these in vitro results suggest the nature of the alkyl ether group may be key to producing TSPO ligands within this class which are functionally active at glioblastomas. The aim of the current work was to examine the cytostatic and cytotoxic properties of DPA-713 and DPA-714 on a human glioblastoma cell line that endogenously expresses the wild type TSPO (Narlawar *et al.*, 2015), and to use a recently described library of alkyl ether analogues of DPA-713 (Reynolds *et al.*, 2010; Banister *et al.*, 2015) to characterize the effect of the alkyl ether chain of DPA-713 on the anti-glioblastoma properties of this chemotype.

2. METHOD:

2.1 Cell culture

The human glioblastoma cell line, T98G, and the human fetal glial cell line, SVG p12, were kindly donated by A/Prof. Lou Rendina (School of Chemistry, University of Sydney). T98G cells were maintained in Dulbecco's modified Eagle's medium: Ham's Nutrient Mixture F-12 (Invitrogen, Carlsbad, CA) and supplemented with 10% heat-inactivated fetal bovine serum (Invitrogen; 10% DMEM/F12). SVGp12 cells were maintained in Minimum Essential Medium (Invitrogen) supplemented with 10% heat-inactivated fetal bovine serum (10% MEM). Once cells reached the exponential phase of growth they were washed with phosphate-buffered saline (PBS, Sigma-Aldrich, St. Louis, MO) and were detached with 0.25 % trypsin (w/v) / 0.02 % ethylenediaminetetraacetic acid (EDTA) (w/v). Cells were plated at a density of 1 x 10^4 cells/well in 96-well plates (Falcon Bioquest, Cockeysville, MD) and allowed to attach for 24 h before assaying.

2.2 Compounds

PK 11195 was purchased from Sigma-Aldrich. DPA-713, DPA-714 and compounds **1-7** (Table 1) were synthesised using described methodology (Reynolds *et al.*, 2010; Banister *et al.*, 2012; Banister *et al.*, 2015). All compounds were dissolved in dimethyl sulfoxide (DMSO; Sigma-Aldrich) and for viability, proliferation, apoptosis and mitochondrial membrane potential assays, compounds were further diluted in 10% DMEM/F12 or 10% MEM. The final DMSO concentration was either 0.1% (PK 11195, DPA-713, compounds **1, 3** and **4**) or 0.2 % (DPA-714, **2**, **5**, **6** and **7**), depending on solubility. DMSO at 0.1 % and 0.2 % did not significantly affect results in any of the functional assays. Cells were treated with at a range of concentrations (1 µM, 10 µM, 25 µM, 50 µM, 75 µM and 100 µM), or treated with vehicle control (0.1% or 0.2% DMSO) (v/v). Treated cells were incubated for 48 h in 5% CO_2 at 37°C for proliferation, viability and apoptosis assays, and were incubated for 6 h and 24 h in the mitochondrial membrane potential assay.

2.3 Radioligand binding

2.3.1 Membrane preparation

For crude membrane preparation, T98G cells were grown to confluence and harvested using phosphate-buffered saline, supplemented with 0.04 % EDTA (w/v), pH 7.4. Cells were spun at 1000 *g* for 10 min and the pellet was suspended in 3 ml of ice-cold 5 mM Tris-HCl (pH 7.4) containing a protease inhibitor cocktail (1:100; Sigma-Aldrich). Cells were homogenised with a hand held Ultra-Turrax homogeniser (IKA Werke, Staufen, Germany). The homogenate was centrifuged at 48,000 *g* for 15 min at 4°C and the supernatant was discarded. The obtained pellet was resuspended in 10 ml of 50 mM Tris-HCl (pH 7.4; binding assay buffer), containing the protease inhibitor cocktail. The homogenate was re-pelleted by centrifugation at 48,000 *g* for 15 min at 4 °C. The pellet was washed once with binding assay buffer and an additional centrifugation step followed where the homogenate was spun at 48000 *g* for 15 min at 4 °C. Total protein in the resulting cell membrane pellet was determined using the bicinchoninic acid protein assay (Pierce Biotechnology Inc., Rockford, IL) according to the manufacturer's protocol.

2.3.2 Saturation binding

T98G cell membranes (20 μg/well diluted in 50 mM Tris-HCl, pH 7.4) were incubated with [^{3}H] PK 11195 (Perkin-Elmer, Beaconsfield, UK) at seven concentrations between 0.1 – 24 nM, in the presence of 3 μM unlabelled PK 11195 (Sigma-Aldrich) to establish non-specific binding, or a vehicle control (1.4 % DMSO) (v/v) to establish total binding. The reaction was incubated for 90 min at 4 °C to achieve equilibrium, terminated by rapid filtration through a glass-fibre filter (GF/C; Millipore, Carrigtwonhill, Ireland) and washed with 50 mM Tris-HCl (pH 7.4), at 4 °C. The filters were then allowed to dry overnight, and covered with Microscint-0 scintillation cocktail (Perkin-Elmer). The amount of radioactivity retained on the filters was determined using a Microbeta2 2450 Microplate Counter (Perkin-Elmer).

2.3.3 Competition binding

T98G cell membranes (20 μg/well) and [^{3}H] PK 11195 (Perkin-Elmer) at 12 nM (K_d determined in 2.3.1) were incubated with 3 μM of PK 11195 (Sigma-Alrich) to assess non-specific binding, a vehicle control (DMSO 1.4 % (v/v)) to establish total binding, and test compounds at ten concentrations between 0.1 – 3162 nM. The reaction was incubated for 90 min at 4 °C. The incubation was terminated by rapid filtration through a glass-fibre filter (Millipore) and washed with 50 mM Tris-HCl (pH 7.4) at 4 °C. The filter was then covered with scintillation cocktail (Perkin-Elmer). The amount of radioactivity retained on the filters was determined using a Microbeta2 2450 Microplate Counter (Perkin-Elmer).

2.4 Cell proliferation assay

5-bromo-2'-deoxyuridine (BrdU) is incorporated into DNA as a substitute for thymidine during cell proliferation. After cells proliferate in the presence of BrdU, detection of BrdU in DNA using an ELISA (Roche Molecular Diagnostics, Indianapolis, IN) can be used as an index of proliferation. After 48 h of exposure to compounds, cells were incubated with 10 μL of BrdU (1:100) at 37°C for 4 h. Cells were then fixed and DNA was denatured for 30 min. A peroxidase-conjugated anti-BrdU antibody (1:100) was subsequently added to the cells for 90 min. The cells were then washed three times with PBS and the substrate solution, 3,3',5,5'-tetramethylbenzidine, was added for 20 min. The reaction was stopped with 1 M sulfuric acid

and the absorbance was measured on a POLARstar Omega plate reader (BMG Labtech) at 450 nm.

2.5 Cell viability assay

Viable cells will metabolise the dye resazurin to the fluorescent molecule resorufin. Measuring the fluorescence from resorufin can be used to compare the number of viable cells across different conditions. Following 48 h of drug treatment, 20 μL of resazurin-containing CellTiter Blue (Promega, Madison, WI) was added to cells and incubated for 4 h in 5 % CO_2, at 37 °C. The supernatant (100 μL) was then transferred to a black-well plate and fluorescence was measured on a POLARstar Omega plate reader (BMG Labtech, Durham, NC) at Ex560/Em590 nm.

2.6 Apoptosis assay

During apoptosis, DNA is cleaved generating mono- and oligo-nucleosomes. The Cell Death ELISA (Roche Molecular Diagnostics) uses antibodies to detect the presence of these nucleosomes. This assay was conducted following 48 h cell treatment. A streptavidin-coated 96-well plate was coated with a biotinylated anti-histone antibody (1:100) and incubated for 1 h. Cells were lysed, incubation media collected, spun at 200 *g* for 10 min and the supernatant collected. The coated 96-well plate was washed three times with PBS and supernatants were added for 90 min. The plate was washed again and a peroxidase-conjugated anti-DNA antibody (1:100) was added for 90 min. After a subsequent wash the substrate solution, 3-ethylbenzothiazoline-6-sulphonic acid, was added for 20 min. The absorbance was read on a POLARstar Omega plate reader (BMG Labtech) at 405 nm.

2.7 Dissipation of mitochondrial membrane potential

Healthy mitochondria maintain a mitochondrial transmembrane potential ($\Delta\Psi_{m)}$, allowing the synthesis of ATP. Cells in the early stage of the intrinsic pathway of apoptosis show a dissipation of $\Delta\Psi_m$ and will not accumulate a fluorescent MitoPotential Dye that otherwise shows high fluorescence in healthy cells. Furthermore, dead cells which have lost membrane structural integrity will uptake the fluorescent dead cell marker 7-AAD. The Muse MitoPotential assay uses flow cytometry to assess the portion of cells that have accumulated MitoPotential Dye and/or 7-AAD, to classify cells as live, live but with dissipated $\Delta\Psi_m$, dead with dissipated $\Delta\Psi_m$ and dead.

T98G cells were plated at $5x10^4$ cells per well of a 48-well plate in 250 μl per well of 10% DMEM/F12. Twenty-four hours after plating, 100 μM compounds or vehicle were added to cells and left for 6 or 24 h. After incubation, the supernatant was collected and cells were washed in 200 μl PBS which was collected. Cells were exposed to 200 μl of 0.25 % trypsin (w/v) / 0.02 % ethylenediaminetetraacetic acid (EDTA) (w/v) for 10 min at 37 degrees, then washed with 350 μl 10% DMEM/F12. The trypsin and media were pooled with the solutions already collected and were spun at 1200 rpm for 5 min. The supernatant was discarded and cells were resuspended in 10% DMEM/F12 at $5x10^5$ cells per ml. One hundred microliters of cell suspension were added to 95 μl of a 1:1000 dilution of Muse MitoPotential Dye diluted in assay buffer. This was incubated for 20 min at 37°C, then 5 ul of 7-AAD was added. After a 10 min incubation, cells were acquired by the Muse cell analyzer and the percentage of each cell state was analysed according to the manufacturer's protocol.

2.8 Microscopy

After 48 h drug treatment (100 μM), morphological changes were documented using differential interference contrast (DIC) microscopy. A Zeiss Axio Observer Live Cell Imaging System (Zeiss, Göttingen, Germany) was used, with the objective lens A-Plan 10x/0.25 Ph1. Cells were imaged in optimal conditions, at 37 °C and 5 % CO2.

2.9 Statistical analysis

All assay conditions were tested in triplicates and means were calculated. Each condition was tested on at least three independent occasions and final mean and standard deviation (SD) values were determined. GraphPad Prism 5 (GraphPad Software Inc., San Diego, CA, U.S.A.) was used for statistical analysis. Saturation binding was analyzed using a non-linear regression curve fit to determine the K_d and B_{max}. Competition binding was analyzed with a four-parameter non-linear regression curve fit to identify the K_i for each compound. The sum of squares F-test was used to assess whether a one or two-site model best fit the competition data. For the viability, proliferation, and apoptosis assays, average basal absorbance for each condition was subtracted to remove background readings. To compare group means in these assays, as well as in the mitochondrial membrane potential assay, a one-way analysis of variance (ANOVA) with a post-hoc Dunnett's test was used. In addition, a Sidak's multiple comparisons test was used to compare proliferation levels in T98G and SVG p12 cells. Statistically significant differences were considered as $p<0.05$. Data is expressed as mean ± standard deviation (SD).

3. RESULTS

3.1 Radioligand binding

The binding of the ligand [^{3}H]-PK 11195 to T98G membranes yielded an equilibrium dissociation constant (K_d) of 11.5 ± 1.2 nM and maximum number of binding sites (B_{max}) of 1132.3 ± 187.7 fmol/mg protein. All compounds bound to TSPO with low nanomolar affinity with the rank order of affinity appearing independent of the nature and length of the R-substituent (Table 1). The sums of squares F-test rejected a two-site model for each of the compounds in favour of a one-site fit.

3.2 Cell proliferation

Measurement of BrdU incorporation using an ELISA was used to assess the anti-proliferative effects of these high affinity TSPO ligands in the human glioblastoma cell line T98G. Furthermore, we assessed the anti-proliferative effects of these ligands on the human fetal astroglial cell line SVG p12 which can be used to investigate the undesirable effects of potential anti-glioblastoma agents on non-cancerous glial cell lines (Mehta *et al.*, 2011; Borawska *et al.*,

2014). DPA-713, DPA-714, **1** and **2** did not induce a change in proliferation in either SVG p12 or T98G cells, although **2** could only be assayed at 75 μM due to solubility limitations. **3** and **6** significantly decreased proliferation in both SVG p12 and T98G cells, with proliferation decreased to a similar extent in both cell lines. **4** significantly decreased proliferation in SVG p12 cells, but produced a significantly greater decrease in proliferation in T98G cells. PK 11195, **5** and **7** did not significantly change proliferation in SVG p12 cells, while significantly decreasing proliferation in T98G cells (Figure 1A). These 3 compounds were also the only compounds to dose-dependently decrease proliferation in T98G cells in a manner potent enough for IC50's to be calculated (Figure 1B). **5** decreased proliferation with an IC50 of 64.6 ± 1.6 μM, **7** decreased proliferation with an IC50 of 71.5 ± 0.5 μM and PK 11195 decreased proliferation with an IC50 of 87.3 ± 4.5 μM.

3.3 Cell viability

To gain insight into whether these compounds only produced cytostatic effects, we investigated the effect of these compounds on cell viability and measures of apoptosis. Surprisingly, PK 11195 did not produce any significant decrease in the number of viable T98G cells, despite its ability to decrease proliferation. The pyrazolopyrimidine-derivatives that showed reduced BrdU incorporation also showed reductions in the number of viable cells present after 48 h treatment, albeit their effect was less potent than on BrdU incorporation (Figure 2). **5** and **7** reduced the number of viable cells with IC50's of 75.9 ± 1.5 and 93.7 ± 5.9 μM respectively.

3.4 Apoptosis

We next examined whether decreases in BrdU incorporation and the number of viable cells was due to apoptosis using a Cell Death ELISA which detects mono- and oligo-nucleosomes, representative of DNA fragmentation created during apoptosis. Compounds **3-7** caused a 3 to 4-fold increase in DNA fragmentation at 100 μM compared to vehicle (Figure 3), while PK 11195 had no effect.

3.5 Dissipation of mitochondrial membrane potential

Apoptosis can occur through an intrinsic and extrinsic pathway. One key point of difference between these two pathways is the role of mitochondria, with the intrinsic pathway featuring opening of the mitochondrial permeability transition pore and dissipation of the mitochondrial membrane potential in the early stages of apoptosis (Elmore, 2007). We used flow cytometry to investigate whether any of the pro-apoptotic compounds, as well as PK 11195, dissipated the mitochondrial membrane potential. After 6h of treatment at 100 μM, the two most potent compounds (**5** and **7**) were the only two compounds to induce lowered levels of healthy live cells and more live cells with depolarized mitochondria (Figure 4A). Compounds **3**, **4** and **6**

showed a delayed induction of mitochondrial depolarization, inducing significant decreases in the number of healthy live cells and more live cells with depolarized mitochondria after 24 h of treatment (Figure 4B). In congruence with its lack of induction of apoptosis, PK 11195 did not show any effect on mitochondrial membrane potential (Figure 4).

3.6 Morphology

Different morphological changes were observed in T98G cells treated with 100 μM PK 11195 and compounds **3** - **7**. PK 11195 caused cells to become elongated, spindle-like and extended processes were evident, while cells treated with compounds **3** - **7** showed morphological changes such as rounding and blebbing (Figure 5).

4. DISCUSSION

Extending the length and nature of the alkyl ether substituent of DPA-713 has minimal influence on affinity for human TSPO, with all derivatives binding with low nanomolar affinity, suggesting a steric tolerance of the alkyl ether substituent during binding. Increasing the number of carbons in the alkyl ether substituent, however, creates a functionally diverse group of ligands. Having up to 3 carbons in the alkyl ether substituent leads to a subgroup of ligands that do not have pro-apoptotic and anti-proliferative effects in the human glioblastoma cell line T98G. Increasing the number of carbons to 4 or 5 produces compounds that induce apoptosis after a delayed dissipation of mitochondrial membrane potential, and show anti-proliferative effects in both T98G cells and a human fetal astroglial cell line, SVG p12. The effect on SVG p12 cells indicate 4 or 5 carbon substituents may produce unwanted effects on non-cancer cells, although the extent to which these are TSPO-mediated is not clear as the level of TSPO expression in these cells is currently unknown. Finally, increasing the number of carbons to 6 or 7 produces a subgroup of compounds that show early induction of glioblastoma membrane potential dissipation and apoptosis. These compounds also cause greatly reduced BrdU incorporation in T98G cells in a manner more potent than PK 11195. While it is not clear the extent to which the reduction in BrdU incorporation is due to cytostatic effects given their pronounced cytotoxic effects, these compounds do not affect BrdU incorporation in SVG p12 cells.

The mechanisms behind the diverse functional outcomes of alkyl ether carbon number variation are not clear. Recently, evidence has accumulated suggesting functional activity of TSPO ligands can be predicted by residence time – the amount of time the ligand interacts with TSPO (Costa *et al.*, 2014; Costa *et al.*, 2016). Costa et al (2014) demonstrated that increasing the residence time of a TSPO ligand, PIGA, facilitated the impairment of glioblastoma viability at lower doses and allowed it to dissipate mitochondrial membrane potential at earlier time points (3 – 6 h vs 12- 24 h). The residence time of the pyrazolopyrimidine derivatives in this

present study are unknown, however the induction of mitochondrial membrane potential dissipation by the higher potency compounds at 6 h compared to induction at 24 h by the lower potency compounds mirrors the change in dissipation time seen by lowering PIGA residence time, suggesting that residence time may be a factor that contributes to functional differences in these compounds. Further, residence time has been shown to predict pregnenolone synthesis efficacy in a class of TSPO ligands (Costa *et al.*, 2016). All compounds showing anti-glioblastoma effects in this present study induce pregnenolone release greater than 200% over basal levels, apart from **5** whose effect on pregnenolone release has not been examined (Reynolds *et al.*, 2010; Banister *et al.*, 2015), while all compounds that do not induce anti-glioblastoma effects in this present study stimulated lower pregnenolone levels, apart from **1** (Reynolds *et al.*, 2010; Banister *et al.*, 2015). Hence this may be further evidence that residence time may contribute to the functional diversity of these compounds.

Surprisingly, the high affinity TSPO ligand PK 11195 demonstrated distinctly different anti-glioblastoma properties to the pyrazolopyrimidine acetamide derivatives. PK 11195 did not display cytotoxic properties, with its outcomes restricted to cytostatic effects. Up regulation of TSPO levels increases glioblastoma proliferation, while downregulation has the opposite effect (Chelli *et al.*, 2008; Rechichi *et al.*, 2008), with neither of these interventions affecting viability. Prolonged exposure to PK 11195 can decrease TSPO levels in breast cancer cell lines (Xu *et al.*, 2016), so if PK 11195 has a similar effect on TSPO levels in glioblastoma cells, then it is possible that its distinct effects may be related to its effect on TSPO levels.

The most potent of the pyrazolopyrimidine analogues had micromolar potency, despite their low nanomolar affinity for TSPO. While this may suggest these anti-glioblastoma effects are not through TSPO specific pathways, there is precedent for discrepancies between affinity and potency when examining the anti-cancer effects of TSPO ligands. PK 11195 has a low nanomolar affinity for TSPO, but an EC_{50} of 50-100 μM for anti-proliferative and pro-apoptotic effects on many different glioma cell lines (Zisterer *et al.*, 1998; Chelli *et al.*, 2008; Kugler *et al.*, 2008). The anti-proliferative and mitochondrial stressor effect of high micromolar concentrations of PK 11195 was prevented by TSPO silencing (Chelli *et al.*, 2008), suggesting these effects were mediated through TSPO. Also, a recently described 4-phenyl quinazoline-2-carboxamide with high affinity for the TSPO decreased U343 glioblastoma viability at micromolar concentrations without off-target activation of G-proteins or a panel of thirteen human kinases linked to glioblastoma (Castellano *et al.*, 2014). Interestingly, even though many TSPO ligands have micromolar potencies in anti-cancer assays *in vitro*, they are still effective at restricting tumor progression *in vivo* (Xia *et al.*, 2000; Decaudin *et al.*, 2002; Shoukrun *et al.*, 2008).

The affinity of compound **1** for human TSPO was comparable to TSPO extracted from rat kidney mitchondria (Reynolds *et al.*, 2010; Banister *et al.*, 2015), however affinities for DPA-713, DPA-714 and the other pyrazolopyrimidine acetamide derivatives differed by two- to eleven-fold from this study. The K_i of DPA-713 in our study more closely resembled the affinity found on binding of [^{3}H]-DPA-713 to human TSPO from monocytic THP-1 cells (Gent *et al.*, 2014). Although the amino acid sequence of TSPO is highly conserved between species (Farges *et al.*, 1994), differences in affinity for rat and human TSPO have been reported for other classes of heteroaromatic TSPO ligands, such as pyrrolobenzoxazepines (Scarf *et al.*, 2012). Given the structural similarity between the pyrrolobenzoxazepines and the pyrazolopyrimidines evaluated in the present study, species differences in TSPO affinity might be expected. This also suggests that small differences in amino acid sequence between rat and human TSPO may profoundly modulate ligand binding.

[^{123}I]-DPA-713 and [^{18}F]-DPA-714 were recently used in single-photon emission computed tomography (SPECT) and positron emission tomography (PET) respectively, to image glioma in pre-clinical murine models (Tang *et al.*, 2012; Winkeler *et al.*, 2012; Awde *et al.*, 2013; O'Brien *et al.*, 2014). These compounds did not affect glioblastoma and astroglial cell proliferation or survival in our assays, highlighting their potential utility as clinical glioblastoma imaging candidates. Results from the current study also suggest that **1** may be a more suitable glioblastoma imaging candidate given its lack of functional activity and relatively higher TSPO affinity compared to DPA-713 and DPA-714.

5. CONCLUSIONS

In summary, we have shown that nine pyrazolo[1,5-*a*]pyridine acetamides substituted with variously alkyl ethers demonstrate nanomolar affinity to human TSPO, indicating that further exploration of the ether group of this chemotype is warranted and likely to be tolerated. By extending the alkyl ether chain we have produced a functionally diverse class of derivatives, some of which induce pro-apoptotic and potentially cytostatic effects on human glioblastoma cells without affecting human astroglial cells. While these ligands may not be candidate therapeutics, future development of this class as potential therapeutic agents for the treatment of glioblastoma could focus on further exploration and structural diversification of the alkyl ether substituent.

ACKNOWLEDGEMENTS

Work presented herein was supported in part by the European Union's Seventh Framework Programme [FP7/2007-2013] INMiND (Grant agreement No. HEALTH-F2-2011-278850). We wish to acknowledge Dr Sandra Fok (Brain and Mind Research Institute) for technical assistance with microscopy. We wish to acknowledge Dr Donna Lai and Dr Sheng Hua (Bosch Molecular Biology Facility) for assistance with use of the Bosch Molecular Biology Facility's equipment.

REFERENCES

Arlicot N, Vercouillie J, Ribeiro MJ, Tauber C, Venel Y, Baulieu JL*, et al.* (2012). Initial evaluation in healthy humans of [18F]DPA-714, a potential PET biomarker for neuroinflammation. *Nuclear medicine and biology* 39**:** 570-578.

Austin CJ, Kahlert J, Kassiou M, Rendina LM (2013). The translocator protein (TSPO): a novel target for cancer chemotherapy. *The international journal of biochemistry & cell biology* 45**:** 1212-1216.

Awde AR, Boisgard R, Theze B, Dubois A, Zheng J, Dolle F*, et al.* (2013). The translocator protein radioligand 18F-DPA-714 monitors antitumor effect of erufosine in a rat 9L intracranial glioma model. *Journal of nuclear medicine : official publication, Society of Nuclear Medicine* 54**:** 2125-2131.

Banati RB, Middleton RJ, Chan R, Hatty CR, Wai-Ying Kam W, Quin C*, et al.* (2014). Positron emission tomography and functional characterization of a complete PBR/TSPO knockout. *Nature communications* 5**:** 5452.

Banister SD, Wilkinson SM, Hanani R, Reynolds A, Hibbs D, Kassiou M (2012). A practical, multigram synthesis of the 2-2(-4-alkoxyphenyl)-5,7-dimethylpyrazolo[1,5-a]pyrimidin-3-yl)acetamide (DPA) class of high affinity translocator protein (TSPO) ligands. *Tetrahedron Letters* 53**:** 3780-3783.

Banister SD, Beinat C, Wilkinson SM, Shen B, Bartoli C, Selleri S*, et al.* (2015). Ether analogues of DPA-714 with subnanomolar affinity for the translocator protein (TSPO). *European journal of medicinal chemistry* 93**:** 392-400.

Borawska MH, Markiewicz-Zukowska R, Naliwajko SK, Moskwa J, Bartosiuk E, Socha K*, et al.* (2014). The interaction of bee products with temozolomide in human diffuse astrocytoma, glioblastoma multiforme and astroglia cell lines. *Nutr Cancer* 66**:** 1247-1256.

Castellano S, Taliani S, Viviano M, Milite C, Da Pozzo E, Costa B*, et al.* (2014). Structure-activity relationship refinement and further assessment of 4-phenylquinazoline-2-carboxamide translocator protein ligands as antiproliferative agents in human glioblastoma tumors. *Journal of medicinal chemistry* 57**:** 2413-2428.

Chauveau F, Boutin H, Van Camp N, Dolle F, Tavitian B (2008). Nuclear imaging of neuroinflammation: a comprehensive review of [11C]PK11195 challengers. *European journal of nuclear medicine and molecular imaging* 35**:** 2304-2319.

Chelli B, Salvetti A, Da Pozzo E, Rechichi M, Spinetti F, Rossi L*, et al.* (2008). PK 11195 differentially affects cell survival in human wild-type and 18 kDa translocator protein-silenced ADF astrocytoma cells. *Journal of cellular biochemistry* 105**:** 712-723.

Corcia P, Tauber C, Vercoullie J, Arlicot N, Prunier C, Praline J*, et al.* (2012). Molecular imaging of microglial activation in amyotrophic lateral sclerosis. *PloS one* 7**:** e52941.

Costa B, Da Pozzo E, Giacomelli C, Barresi E, Taliani S, Da Settimo F*, et al.* (2016). TSPO ligand residence time: a new parameter to predict compound neurosteroidogenic efficacy. *Scientific reports* 6**:** 18164.

Costa B, Da Pozzo E, Giacomelli C, Taliani S, Bendinelli S, Barresi E*, et al.* (2014). TSPO ligand residence time influences human glioblastoma multiforme cell death/life balance. *Apoptosis : an international journal on programmed cell death*.

Coughlin JM, Wang Y, Ma S, Yue C, Kim PK, Adams AV*, et al.* (2014). Regional brain distribution of translocator protein using [(11)C]DPA-713 PET in individuals infected with HIV. *Journal of neurovirology* 20**:** 219-232.

Decaudin D, Castedo M, Nemati F, Beurdeley-Thomas A, De Pinieux G, Caron A*, et al.* (2002). Peripheral benzodiazepine receptor ligands reverse apoptosis resistance of cancer cells in vitro and in vivo. *Cancer research* 62**:** 1388-1393.

Elmore S (2007). Apoptosis: a review of programmed cell death. *Toxicol Pathol* 35**:** 495-516.

Endres CJ, Coughlin JM, Gage KL, Watkins CC, Kassiou M, Pomper MG (2012). Radiation dosimetry and biodistribution of the TSPO ligand 11C-DPA-713 in humans. *Journal of nuclear medicine : official publication, Society of Nuclear Medicine* 53**:** 330-335.

Endres CJ, Pomper MG, James M, Uzuner O, Hammoud DA, Watkins CC*, et al.* (2009). Initial evaluation of 11C-DPA-713, a novel TSPO PET ligand, in humans. *Journal of nuclear medicine : official publication, Society of Nuclear Medicine* 50**:** 1276-1282.

Farges R, Joseph-Liauzun E, Shire D, Caput D, Le Fur G, Ferrara P (1994). Site-directed mutagenesis of the peripheral benzodiazepine receptor: identification of amino acids implicated in the binding site of Ro5-4864. *Molecular pharmacology* 46**:** 1160-1167.

Gent YY, Weijers K, Molthoff CF, Windhorst AD, Huisman MC, Kassiou M*, et al.* (2014). Promising potential of new generation translocator protein tracers providing enhanced contrast of arthritis imaging by positron emission tomography in a rat model of arthritis. *Arthritis research & therapy* 16**:** R70.

Ikezaki K, Black KL (1990). Stimulation of cell growth and DNA synthesis by peripheral benzodiazepine. *Cancer letters* 49**:** 115-120.

James ML, Fulton RR, Vercoullie J, Henderson DJ, Garreau L, Chalon S*, et al.* (2008). DPA-714, a new translocator protein-specific ligand: synthesis, radiofluorination, and pharmacologic characterization. *Journal of nuclear medicine : official publication, Society of Nuclear Medicine* 49**:** 814-822.

Johnson DR, O'Neill BP (2012). Glioblastoma survival in the United States before and during the temozolomide era. *Journal of neuro-oncology* 107**:** 359-364.

Kugler W, Veenman L, Shandalov Y, Leschiner S, Spanier I, Lakomek M*, et al.* (2008). Ligands of the mitochondrial 18 kDa translocator protein attenuate apoptosis of human glioblastoma cells exposed to erucylphosphohomocholine. *Cellular oncology : the official journal of the International Society for Cellular Oncology* 30**:** 435-450.

Mehta A, Shervington L, Munje C, Shervington A (2011). A novel therapeutic strategy for the treatment of glioma, combining chemical and molecular targeting of hsp90a. *Cancers (Basel)* 3**:** 4228-4244.

Miettinen H, Kononen J, Haapasalo H, Helen P, Sallinen P, Harjuntausta T*, et al.* (1995). Expression of peripheral-type benzodiazepine receptor and diazepam binding inhibitor in human astrocytomas: relationship to cell proliferation. *Cancer research* 55**:** 2691-2695.

Miyazawa N, Hamel E, Diksic M (1998). Assessment of the peripheral benzodiazepine receptors in human gliomas by two methods. *Journal of neuro-oncology* 38**:** 19-26.

Narlawar R, Werry EL, Scarf AM, Hanani R, Chua SW, King VA*, et al.* (2015). First Demonstration of Positive Allosteric-like Modulation at the Human Wild Type Translocator Protein (TSPO). *Journal of medicinal chemistry* 58**:** 8743-8749.

O'Brien ER, Kersemans V, Tredwell M, Checa B, Serres S, Soto MS*, et al.* (2014). Glial activation in the early stages of brain metastasis: TSPO as a diagnostic biomarker. *Journal of nuclear medicine : official publication, Society of Nuclear Medicine* 55**:** 275-280.

Omay SB, Vogelbaum MA (2009). Current concepts and newer developments in the treatment of malignant gliomas. *Indian journal of cancer* 46**:** 88-95.

Owen DR, Gunn RN, Rabiner EA, Bennacef I, Fujita M, Kreisl WC*, et al.* (2011). Mixed-affinity binding in humans with 18-kDa translocator protein ligands. *Journal of nuclear medicine : official publication, Society of Nuclear Medicine* 52**:** 24-32.

Papadopoulos V, Baraldi M, Guilarte TR, Knudsen TB, Lacapere JJ, Lindemann P*, et al.* (2006). Translocator protein (18kDa): new nomenclature for the peripheral-type benzodiazepine receptor based on its structure and molecular function. *Trends in pharmacological sciences* 27**:** 402-409.

Rechichi M, Salvetti A, Chelli B, Costa B, Da Pozzo E, Spinetti F*, et al.* (2008). TSPO over-expression increases motility, transmigration and proliferation properties of C6 rat glioma cells. *Biochimica et biophysica acta* 1782**:** 118-125.

Reynolds A, Hanani R, Hibbs D, Damont A, Da Pozzo E, Selleri S*, et al.* (2010). Pyrazolo[1,5-a]pyrimidine acetamides: 4-Phenyl alkyl ether derivatives as potent ligands for the 18 kDa translocator protein (TSPO). *Bioorganic & medicinal chemistry letters* 20**:** 5799-5802.

Scarf AM, Luus C, Da Pozzo E, Selleri S, Guarino C, Martini C*, et al.* (2012). Evidence for complex binding profiles and species differences at the translocator protein (TSPO) (18 kDa). *Current molecular medicine* 12**:** 488-493.

Selleri S, Bruni F, Costagli C, Costanzo A, Guerrini G, Ciciani G*, et al.* (2001). 2-Arylpyrazolo[1,5-a]pyrimidin-3-yl acetamides. New potent and selective peripheral benzodiazepine receptor ligands. *Bioorganic & medicinal chemistry* 9**:** 2661-2671.

Shoukrun R, Veenman L, Shandalov Y, Leschiner S, Spanier I, Karry R*, et al.* (2008). The 18-kDa translocator protein, formerly known as the peripheral-type benzodiazepine receptor, confers proapoptotic and antineoplastic effects in a human colorectal cancer cell line. *Pharmacogenetics and genomics* 18**:** 977-988.

Su Z, Herholz K, Gerhard A, Roncaroli F, Du Plessis D, Jackson A*, et al.* (2013). [(1)(1)C]-(R)PK11195 tracer kinetics in the brain of glioma patients and a comparison of two referencing approaches. *European journal of nuclear medicine and molecular imaging* 40**:** 1406-1419.

Tang D, Hight MR, McKinley ET, Fu A, Buck JR, Smith RA*, et al.* (2012). Quantitative preclinical imaging of TSPO expression in glioma using N,N-diethyl-2-(2-(4-(2-18F-fluoroethoxy)phenyl)-5,7-dimethylpyrazolo[1,5-a]pyrimi din-3-yl)acetamide. *Journal of nuclear medicine : official publication, Society of Nuclear Medicine* 53**:** 287-294.

Veenman L, Levin E, Weisinger G, Leschiner S, Spanier I, Snyder SH*, et al.* (2004). Peripheral-type benzodiazepine receptor density and in vitro tumorigenicity of glioma cell lines. *Biochemical pharmacology* 68**:** 689-698.

Vlodavsky E, Soustiel JF (2007). Immunohistochemical expression of peripheral benzodiazepine receptors in human astrocytomas and its correlation with grade of malignancy, proliferation, apoptosis and survival. *Journal of neuro-oncology* 81**:** 1-7.

Werry EL, Barron ML, Kassiou M (2015). TSPO as a target for glioblastoma therapeutics. *Biochem Soc Trans* 43**:** 531-536.

Winkeler A, Boisgard R, Awde AR, Dubois A, Theze B, Zheng J*, et al.* (2012). The translocator protein ligand [(1)(8)F]DPA-714 images glioma and activated microglia in vivo. *European journal of nuclear medicine and molecular imaging* 39**:** 811-823.

Xia W, Spector S, Hardy L, Zhao S, Saluk A, Alemane L*, et al.* (2000). Tumor selective G2/M cell cycle arrest and apoptosis of epithelial and hematological malignancies by BBL22, a benzazepine. *Proceedings of the National Academy of Sciences of the United States of America* 97**:** 7494-7499.

Xu JN, Shen D, Mao WD, Lin QF, Lin F, Lu C (2016). The effects of PK11195 on the MCF-7 and T47D were associated with the allopregnanolone biosynthesis, which was mediated by Translocator Protein 18 KDa. *Cancer Biomark* 17**:** 11-16.

Zisterer DM, Hance N, Campiani G, Garofalo A, Nacci V, Williams DC (1998). Antiproliferative action of pyrrolobenzoxazepine derivatives in cultured cells: absence of correlation with binding to the peripheral-type benzodiazepine binding site. *Biochemical pharmacology* 55**:** 397-403.

Table 1. Binding affinities of pyrazolopyrimidine derivatives for TSPO in T98G cells. Values represent the mean ± SD, from three independent experiments.

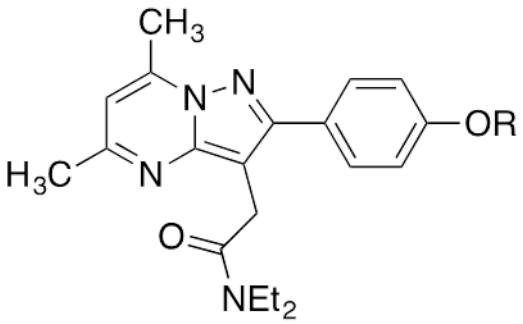

Compound	R	K_i (TSPO) (nM)
PK 11195	-	1.6 ± 0.30
DPA-713	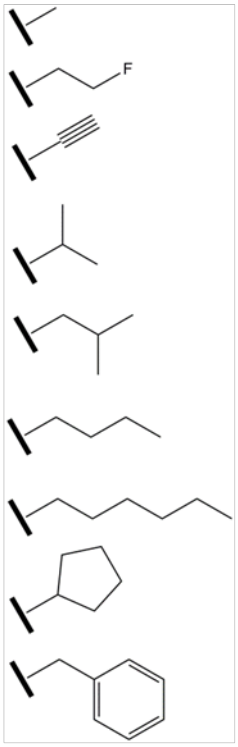	10.4 ± 3.2
DPA-714		11.6 ± 3.7
1		4.9 ± 2.9
2		15.3 ± 11.5
3		16.3 ± 3.4
4		4.8 ± 3.5
5		16.9 ± 6.3
6		21.3 ± 0.6
7		4.3 ± 0.5

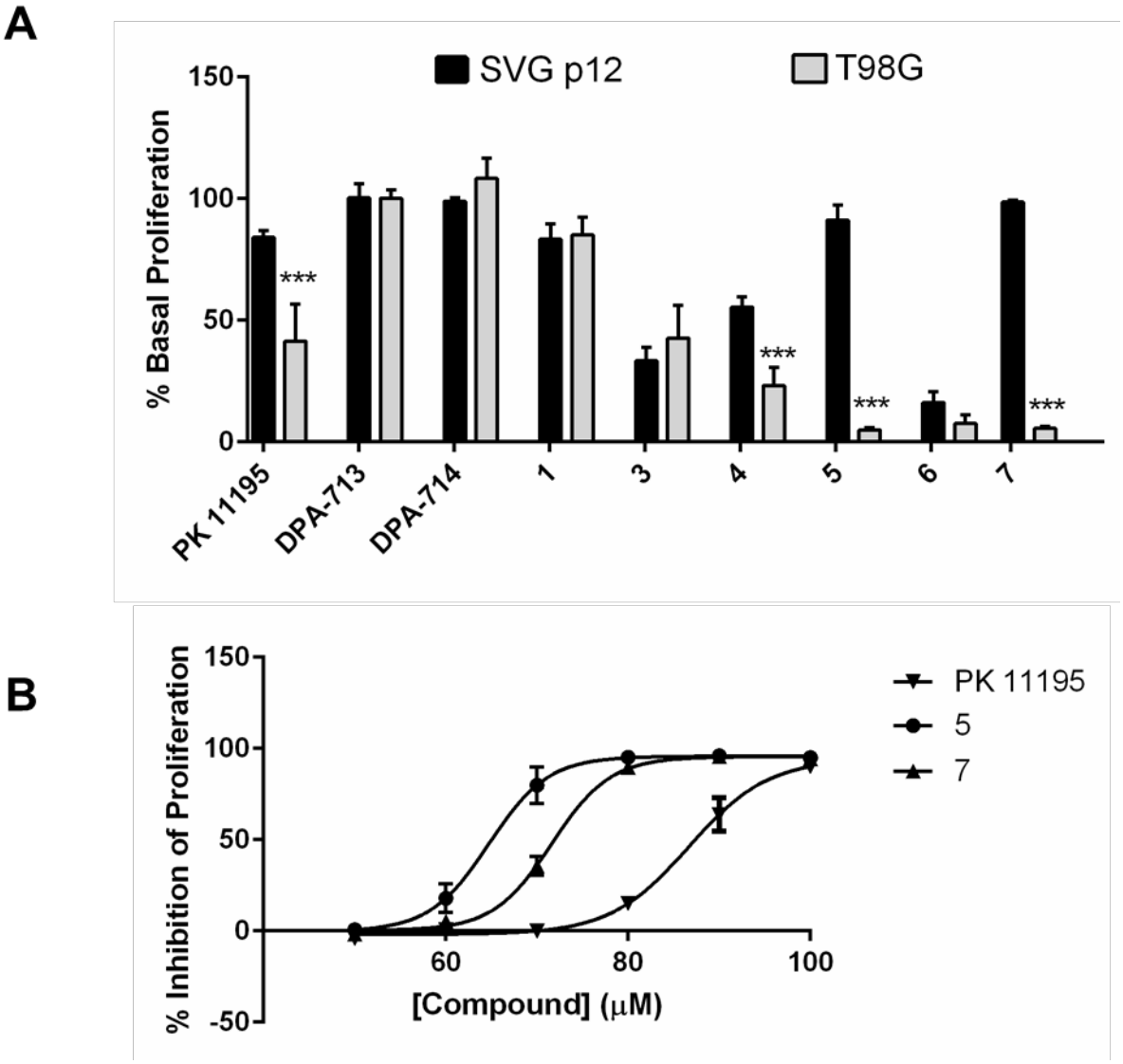

Figure 1. The effect of pyrazolopyrimidine derivatives on SVG p12 and T98G proliferation. Both cell lines were treated for 48 h with 100 μM. ***p<0.001 when percentage of proliferation in T98G cells was compared to that in SVG p12 cells using a one-way ANOVA with Sidak's multiple comparisons test (A). Compounds producing significant decreases in proliferation were further assessed across a range of concentrations (50 – 100 μM), and those potent enough to produce IC50's are displayed in (B). Values represent the mean ± SD, from three independent experiments.

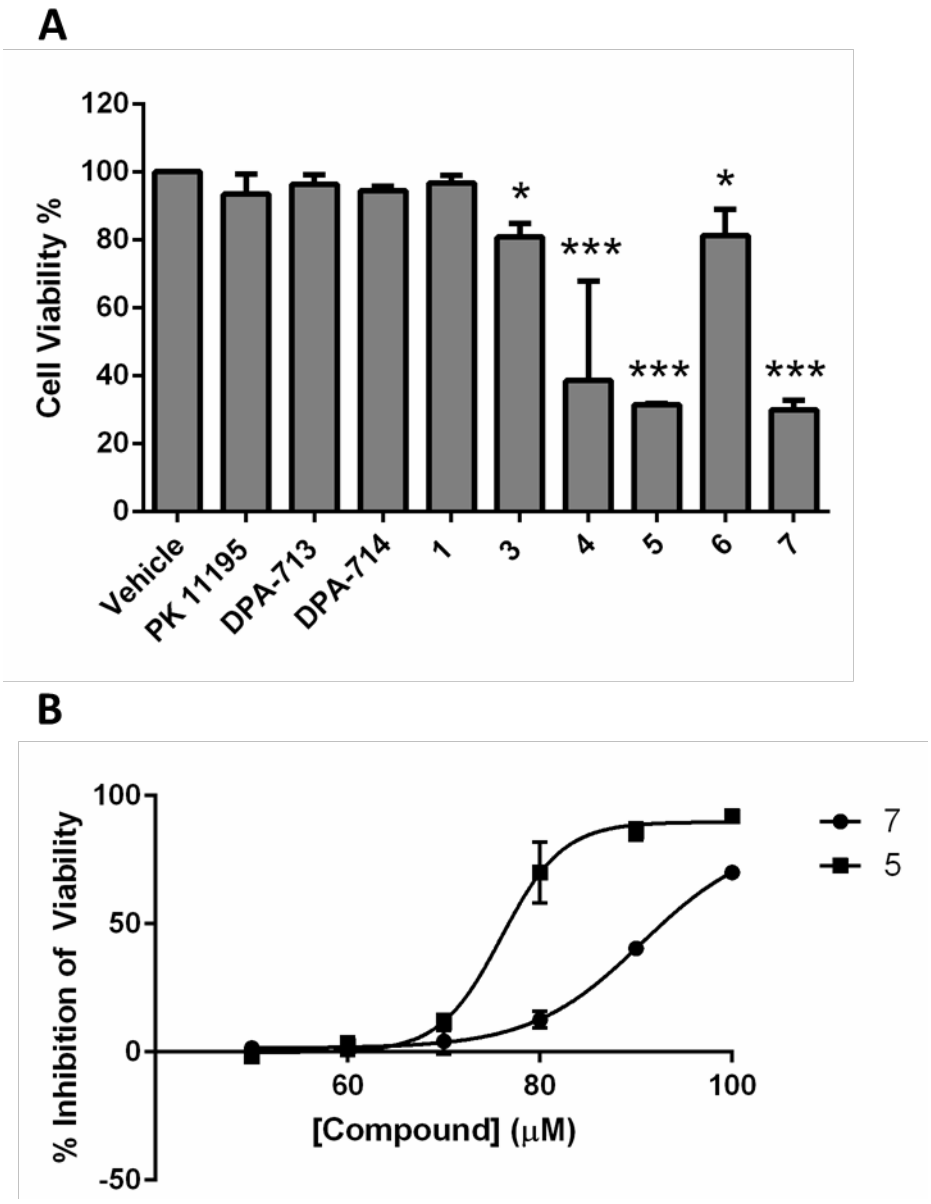

Figure 2. The effect of pyrazolopyrimidine derivatives on T98G viability. T98G cells were treated for 48 h with 100 μM of each compound. *p<0.01, ***p<0.001 when percentage of proliferation in treated T98G cells was compared to that in vehicle-treated cells using a one-way ANOVA with Dunnett's multiple comparisons test (A). Compounds producing significant decreases in proliferation were further assessed across a range of concentrations (50 – 100 μM), and those potent enough to produce IC50's are displayed in (B). Values represent the mean ± SD, from three independent experiments.

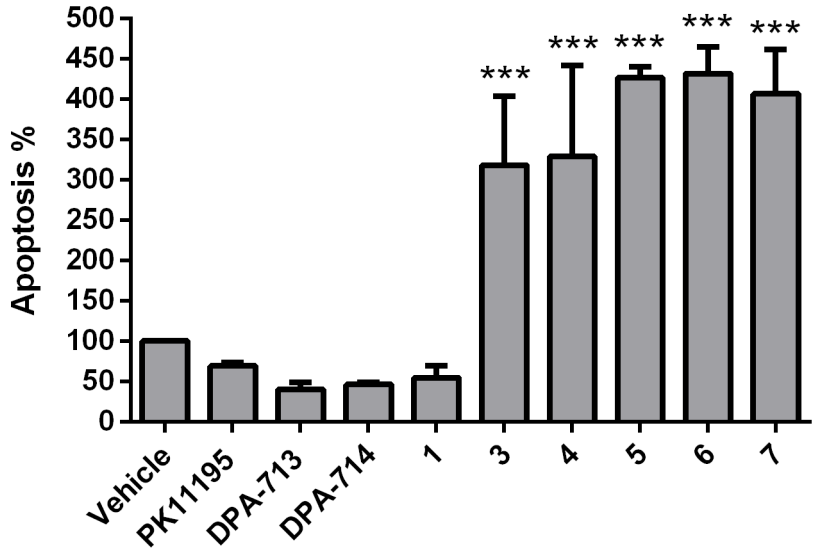

Figure 3. The effect of PK 11195- and pyrazolopyrimidine derivatives on apoptosis in T98G cells. Compounds **3-7** induced a significant level of apoptosis compared to vehicle after 48 h of treatment, as detected by a one-way ANOVA with Dunnett's multiple comparisons test. Values represent the mean percent of vehicle ± SD of at least three experiments. ***$p < 0.001$.

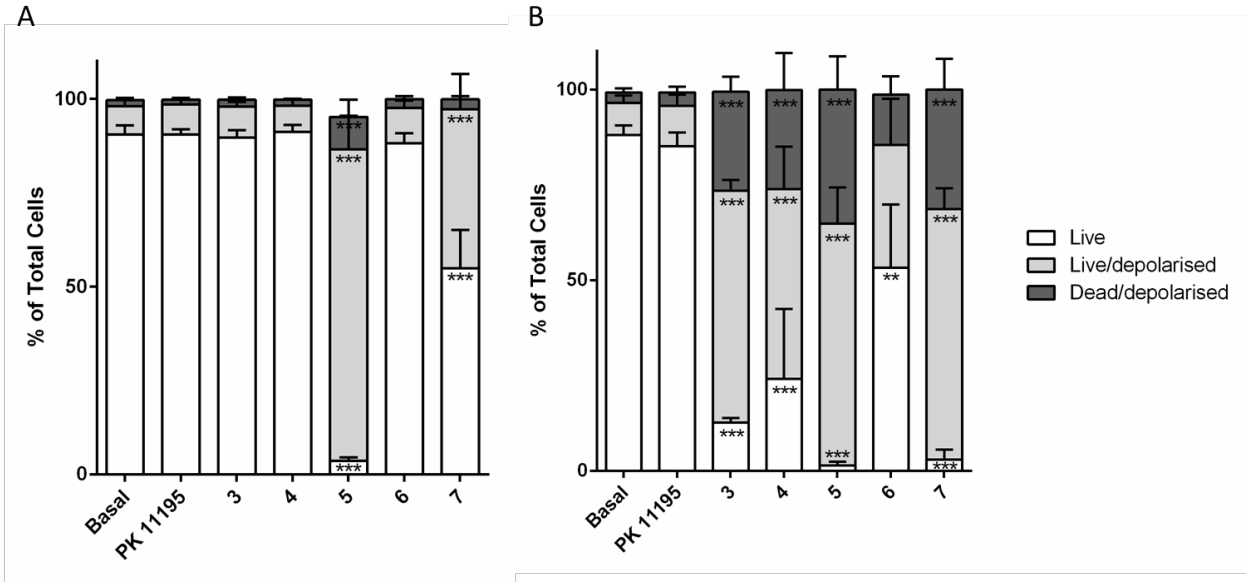

Figure 4. The effect of PK 11195 and pyrazolopyrimidine derivatives on T98G mitochondrial membrane potential ($\Delta\Psi_m$) dissipation. $\Delta\Psi_m$ was assessed after exposure to 100 μM of compounds for (A) 6 h and (B) 24 h. Cells were classified as live, live but depolarized and dead after depolarization. A one-way ANOVA with Dunnett's multiple comparison's test was used to assess significant differences in the mean level of each cell state after treatment compared to the basal levels (**p<0.01, ***p<0.001). Values represent the mean ± SD, from at least three independent experiments.

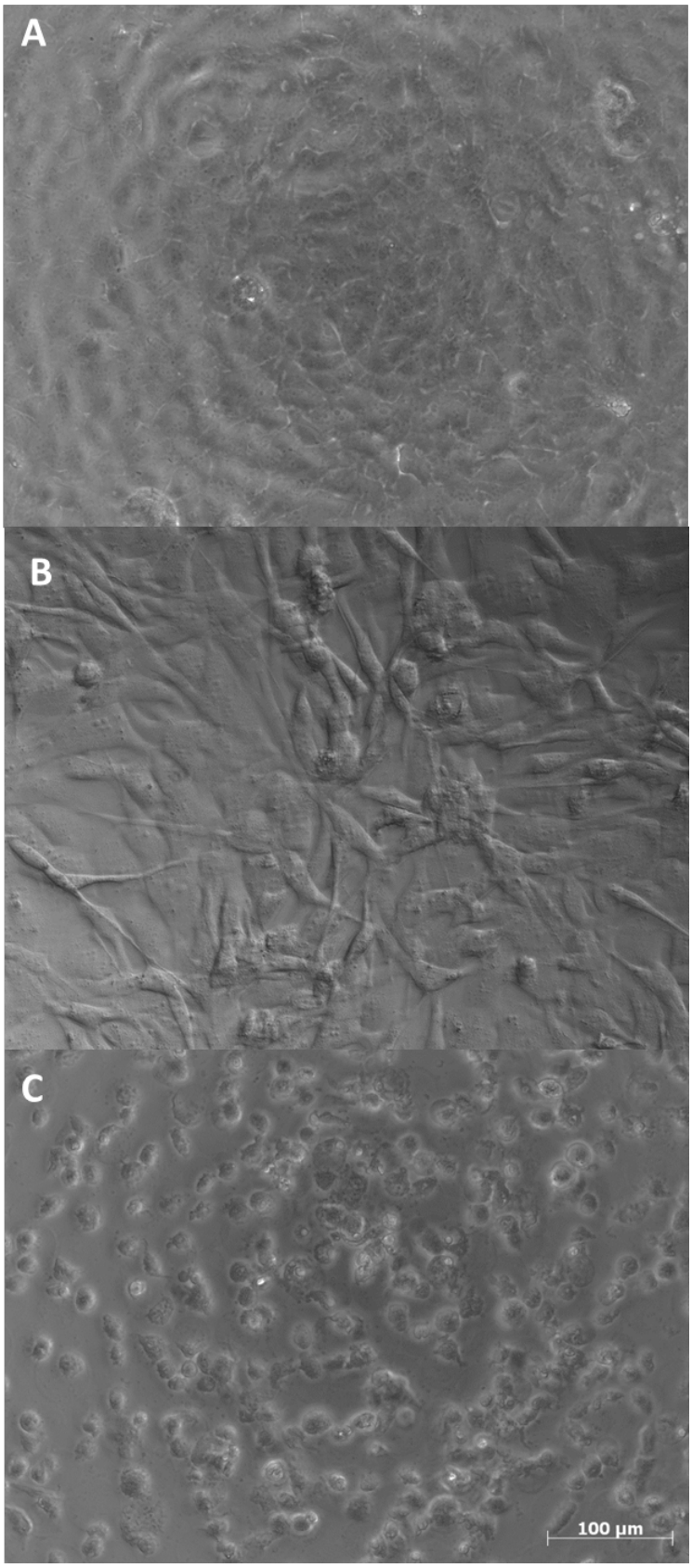
A
B
C
100 µm

Figure 5. The effect of PK 11195 and 4 on T98G morphology. Exposure of cells to 100 μM of vehicle (A), PK 11195 (B) and **4** (C) for 48 h produced distinct morphology changes with PK 11195 inducing a spindle-like morphology while 4 produced rounding and blebbing. Morphology on exposure to **4** was representative of morphology on exposure to **3**, **5**, **6** and **7**.